**Supplemental Information**

# Regulation of Lipids is Central to Replicative Senescence

Darleny Y. Lizardo[1], Yen-Lung Lin[2], Omer Gokcumen[2*], G. Ekin Atilla-Gokcumen[1*]

[1]Department of Chemistry, [2]Department of Biological Sciences, University at Buffalo, The State University of New York (SUNY), Buffalo, NY USA 14260

*Correspondence should be addressed to G.E.A- G. (ekinatil@buffalo.edu) or O.G. (gokcumen@gmail.com)

## Table of Contents

## Supplementary Figures and Tables

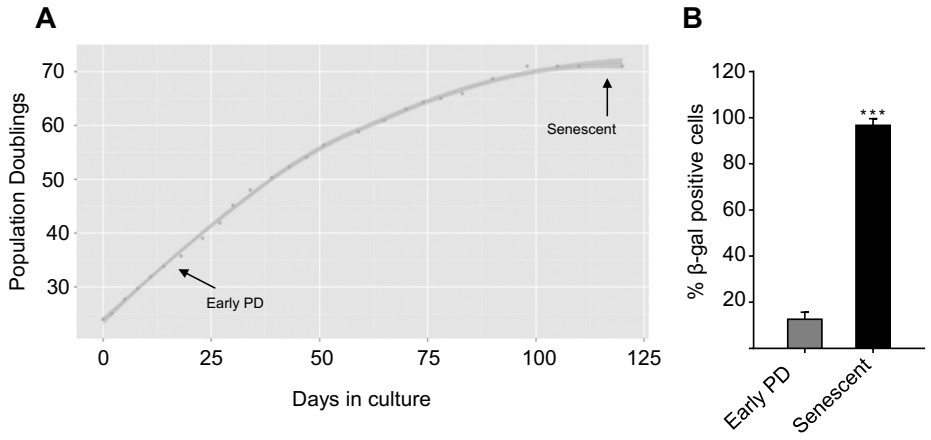


**Figure S1.** Growth curve and characterization of replicative senescence in MRC-5 cells. (A) MRC-5 cells were maintained in culture until they naturally reached their proliferative capacity. For profiling experiments MRC-5 cells at PD ~32 were used as "early PD" cells and cells at PD ~70 were used as "senescent" cells. (B) Measurement of SA-β-gal in early PD and senescent MRC-5 cells. Assay was carried out in three independent experiments, $n \geq 200$ cells for each group (t-test, p value $\leq 0.001$).

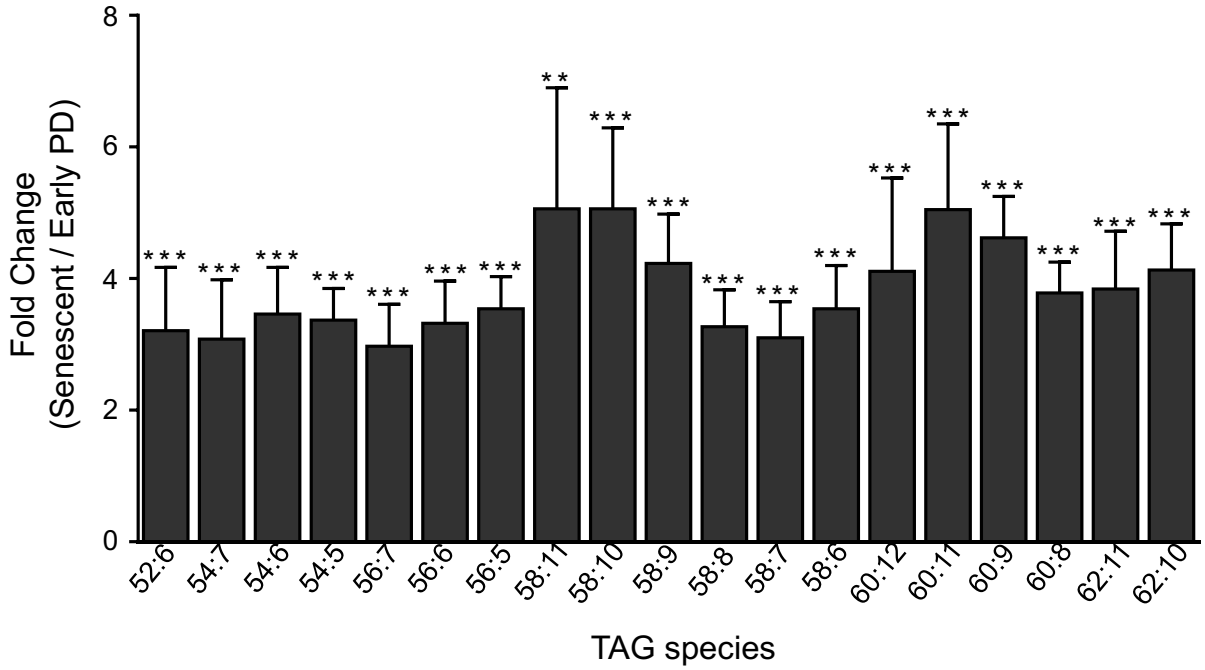


**Figure S2.** Triacylglycerols accumulate during replicative senescence in MRC-5 cells. TAG species identified during our global lipidomics analysis in BJ cells were targeted in early PD and senescent MRC-5 cells. Five biological replicates were used for each experimental condition. Fold change was determined as [Abundance$_{Senescent}$] / [Abundance$_{EarlyPD}$] for each TAG species. Abundance is the total ion counts for a given ion. Each ion corresponds to a mass-to-charge ratio (*m/z*), which is used to assign the TAG species. MS/MS analysis was carried out to confirm TAG structures. (***$p < 0.001$, **$p < 0.01$).

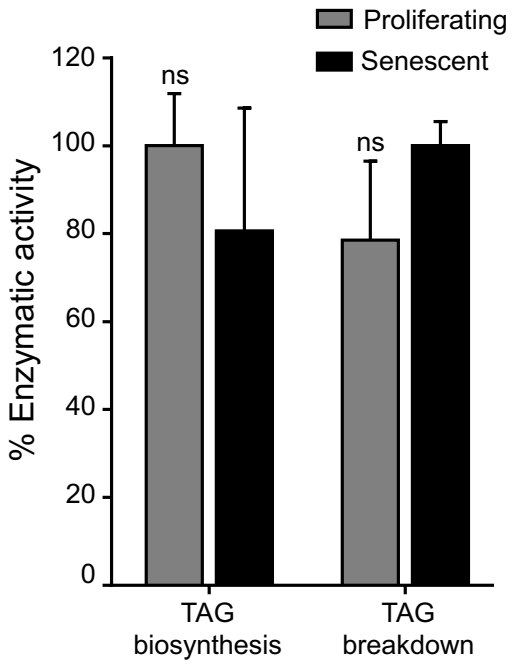


**Figure S3.** Activity of enzymes involved in triacylglycerol (TAG) metabolism. The overall activity of TAG biosynthesis was assessed by measuring the conversion of DAG (14:0/14:0) and fatty acyl CoA (17:0) substrates to the corresponding TAG (14:0,14:0,17:0). Enzymatic activity of TAG breakdown was assessed my measuring the breakdown of TAG (13:0/13:0/13:0) to DAG (13:0/13:0). The activities of enzymes involved in the synthesis or breakdown of TAGs did not change as BJ cells reached the senescent state (ns: not significant).

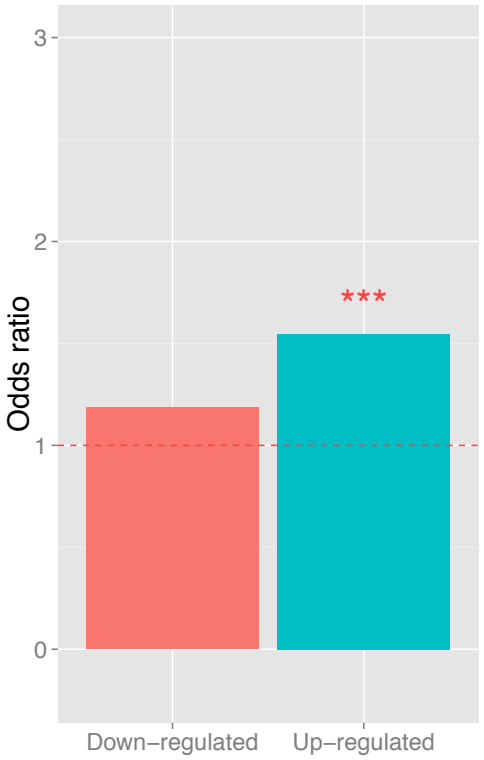


**Figure S4.** A higher number of genes involved in response to oxidative stress are significantly up-regulated in senescent cells as compared to early PD cells. To see whether there is a greater than expected number of oxidative stress response genes being altered during senescence, we calculated the proportion of genes up- or down-regulated in senescent cells. The two bars in the figure represent the enrichment of the significantly up-regulated (cyan) and down-regulated oxidative stress response related genes (red) as compared to the down- and up-regulation of all genes in the genome, respectively. We observed a significant fold enrichment for the number of up-regulated genes; however, we did not observe a significant enrichment for the number of down-regulated genes. The horizontal red dash line indicates a level of odds ratio = 1, which means no enrichment. (***$p < 0.05$ , Fisher's exact test).

**Table S1 (uploaded as Supplemental Table 1).** RNAseq data of protein coding genes. This is provided as a separate excel spreadsheet. The columns are: Ensemble gene ID, HUGO gene names, full gene names, $\log_2$ value of early PD/senescent cell expressional ratio, raw significance of the expressional difference and adjusted significance of the expressional difference, which has been corrected for multiple hypotheses, are provided.

**Table S2 (uploaded as Supplemental Table 2).** List of Gene Ontology (GO) terms enriched with genes that show significant transcriptional difference between early PD and senescent cells are provided in a separate excel spreadsheet. GO enrichment analysis suggests that senescence related genes (genes with significant transcriptional difference between early PD and senescent cells, FDR q-value <0.05) are more commonly seen in these biological processes. GO Term: ID of a GO term; Description: description of the GO term; FDR q-value: significance of enrichment, corrected for multiple hypotheses; Enrichment: fold of enrichment of senescence related genes within this term.

**Table S3.** Thirteen lipid-related biological processes were identified during the GO enrichment analysis. Among the biological processes with an enriched number of senescence related genes, thirteen lipid-related GO terms were identified.

| GO Term | Description | FDR q-value[a] | Enrichment[b] |
|---|---|---|---|
| GO:0006665 | sphingolipid metabolic process | 3.21E-05 | 1.75 |
| GO:0006643 | membrane lipid metabolic process | 1.23E-04 | 1.62 |
| GO:0006644 | phospholipid metabolic process | 2.62E-04 | 1.42 |
| GO:0033993 | response to lipid | 3.88E-04 | 1.27 |
| GO:0006629 | lipid metabolic process | 1.67E-03 | 1.19 |
| GO:0046839 | phospholipid dephosphorylation | 4.52E-03 | 2.17 |
| GO:0044255 | cellular lipid metabolic process | 4.73E-03 | 1.2 |
| GO:0006650 | glycerophospholipid metabolic process | 6.64E-03 | 1.37 |
| GO:0006687 | glycosphingolipid metabolic process | 7.59E-03 | 1.75 |
| GO:0006869 | lipid transport | 8.00E-03 | 1.38 |
| GO:0071396 | cellular response to lipid | 9.50E-03 | 1.33 |
| GO:0008654 | phospholipid biosynthetic process | 1.21E-02 | 1.42 |
| GO:0008610 | lipid biosynthetic process | 1.53E-02 | 1.25 |

[a] FDR q-value: significance of enrichment, corrected for multiple hypotheses. [b] Enrichment: fold of enrichment of senescence related genes within this term.

**Table S4.** Lipid-related pathways from KEGG. Twelve lipid metabolism pathways were selected from KEGG to test whether there is an enrichment of genes that show significant expressional differences between early PD and senescent cells.

| Pathway | # of genes |
|---|---|
| Alpha linolenic acid metabolism | 25 |
| Arachidonic acid metabolism | 62 |
| Ether lipid metabolism | 45 |
| Fatty acid biosynthesis | 13 |
| Fatty acid degradation | 44 |
| Fatty acid elongation | 25 |
| Glycerolipid metabolism | 59 |
| Glycerophospholipid metabolism | 95 |
| Linoleic acid metabolism | 29 |
| Sphingolipid metabolism | 47 |
| Steroid biosynthesis | 20 |
| Unsaturated fatty acid biosynthesis | 23 |

**Table S5 (uploaded as Supplemental Table 5).** Abundances of lipids studied *via* comparative lipidomics. Abundances, *m/z*'s, adducts observed and retention times in each sample for lipids identified in untargeted and targeted analysis are provided in a separate excel spreadsheet. Abbreviations: *m/z*: mass-to-charge ratio; FC: fold change; FA: fatty acid; PA: phosphatidic acid; PE: phosphatidylethanolamine; PC: phosphatidylcholine; PI: phosphatidylinositol; PS: phosphatidylserine; MAG: monoacylglycerol; DAG: diacylglycerol; TAG: triacylglycerol; Cer: ceramide; DiHCer: dihydroceramide. FC was determined as $[Abundance_{Senescent}]$ / $[Abundance_{EarlyPD}]$ for each lipid species. Abundance is the total ion count for a given ion. Background correction for abundant fatty acids has been carried out as necessary. Each ion corresponds to a mass-to-charge ratio (*m/z*). Total carbon number on the acyl chains and the degree of unsaturation of the fatty acyl chains in the lipid species are listed, *i.e.* C38:4 corresponds to 38 carbons and 4 double bonds.

**Supplemental Fragmentation Information and Lipid Assignments of Species Analyzed by Untargeted and Targeted Lipidomics**

Fragmentation information of representative species is reported below.

Identification of Species from Untargeted Lipidomics

**Identification of *m/z* = 868.7367.** Retention time = 68.5. MS/MS fragments obtained were searched in METLIN. Observed fragments: 239.2333, 311.2323, 313.2696, 523.4623, 595.4657, and 623.4942. According to this fragmentation pattern *m/z* = 868.7367, $[M+NH_4]^+$, was identified as TAG (14:0, 16:0, 22:6) ($m/z_{theoretical}$ = 868.7389).

**Identification of *m/z* = 894.7565.** Retention time = 65.3. MS/MS fragments obtained were searched in METLIN. Observed fragments: 237.2186, 311.2381, 313.2715, 549.4872, 621.4885, and 623.5041. According to this fragmentation pattern *m/z* = 894.7565, $[M+NH_4]^+$, was identified as TAG (16:0, 16:1, 22:6) ($m/z_{theoretical}$ = 894.7545).

**Identification of *m/z* = 896.7595.** Retention time = 65.9. MS/MS fragments obtained were searched in METLIN. Observed fragments: 261.2219, 263.2390, 265.2465, 337.2771, 339.2942, 597.4850, 599.5027, and 601.5142. According to this fragmentation pattern *m/z* = 896.7595, $[M+NH_4]^+$, was identified as TAG (18:1, 18:2, 18:3) ($m/z_{theoretical}$ = 896.7702).

**Identification of *m/z* = 898.7716.** Retention time = 66.7. MS/MS fragments obtained were searched in METLIN. Observed fragments: 263.2374, 265.2525, 337.2739, 339.2901, 599.5041, and 601.5162. According to this fragmentation pattern *m/z* = 898.7716, $[M+NH_4]^+$, was identified as TAG (18:1, 18:2, 18:2) ($m/z_{theoretical}$ = 898.7858).

**Identification of *m/z* = 922.7721.** Retention time = 66.4. MS/MS fragments obtained were searched in METLIN. Observed fragments: 265.2475, 311.2339, 313.2696, 339.2849, 577.5163, 623.5047, and 649.5128. According to this fragmentation pattern *m/z* = 922.7721, $[M+NH_4]^+$, was identified as TAG (16:0, 18:1, 22:6) ($m/z_{theoretical}$ = 922.7858).

**Identification of *m/z* = 924.7894.** Retention time = 66.8. MS/MS fragments obtained were searched in METLIN. Observed fragments: 239.2288, 265.2536, 313.2622, 339.2848, 577.5204, 625.5125, and 651.5410. According to this fragmentation pattern *m/z* = 924.7894, $[M+NH_4]^+$, was identified as TAG (16:0, 18:1, 22:5) ($m/z_{theoretical}$ = 924.8015).

**Identification of *m/z* = 926.8216.** Retention time = 66.9. MS/MS fragments obtained were searched in METLIN. Observed fragments: 265.2500, 267.2643, 287.2340, 339.2860, 341.3003, 605.5431, 625.5128, and 627.5284. According to this fragmentation pattern *m/z* = 926.8216, $[M+NH_4]^+$, was identified as TAG (18:0, 18:1, 20:4) ($m/z_{theoretical}$ = 926.8171).

**Identification of *m/z* = 942.7587.** Retention time = 68.0. MS/MS fragments obtained were searched in METLIN. Observed fragments: 265.2484, 285.2206, and 623.5042. According to this fragmentation pattern *m/z* = 942.7587, $[M+NH_4]^+$, was identified as TAG (18:1, 20:5, 20:5) ($m/z_{theoretical}$ = 942.7545).

**Identification of *m/z* = 944.7586.** Retention time = 65.4. MS/MS fragments obtained were searched in METLIN. Observed fragments: 239.2366, 287.2365, 311.2389, 361.2771, 599.5011, 623.5011, and 671.4924. According to this fragmentation pattern *m/z* = 944.7586, $[M+NH_4]^+$, was identified as TAG (16:0, 20:4, 22:6) ($m/z_{theoretical}$ = 944.7702).

**Identification of *m/z* = 946.7717.** Retention time = 66.1. MS/MS fragments obtained were searched in METLIN. Observed fragments: 239.2420, 311.2390, 313.2713, 361.2607, 601.5111, 623.4933, and 673.5050. According to this fragmentation pattern *m/z* = 946.7717, $[M+NH_4]^+$, was identified as TAG (16:0, 20:3, 22:6) ($m/z_{theoretical}$ = 946.7858).

**Identification of *m/z* = 948.7874.** Retention time = 66.5. MS/MS fragments obtained were searched in METLIN. Observed fragments: 265.2478, 311.2346, 339.2780, 603.5170, and 649.4968. According to this fragmentation pattern *m/z* = 948.7874, $[M+NH_4]^+$, was identified as TAG (18:1, 18:1, 22:6) ($m/z_{theoretical}$ = 948.8015).

**Identification of *m/z* = 950.8208.** Retention time = 66.5. MS/MS fragments obtained were searched in METLIN. Observed fragments: 265.2465, 267.2687, 311.2379, 339.2898, 605.5508, and 651.5355. According to this fragmentation pattern *m/z* = 950.8208, $[M+NH_4]^+$, was identified as TAG (18:0, 18:1, 22:6) ($m/z_{theoretical}$ = 950.8171).

**Identification of *m/z* = 952.8383.** Retention time = 66.4. MS/MS fragments obtained were searched in METLIN. Observed fragments: 265.2497, 287.2313, 339.2873, 367.3160, 631.5636, 625.5175, and 653.5468. According to this fragmentation pattern *m/z* = 952.8383, $[M+NH_4]^+$, was identified as TAG (18:1, 20:1, 20:4) ($m/z_{theoretical}$ = 952.8328).

**Identification of *m/z* = 968.7563.** Retention time = 65.1. MS/MS fragments obtained were searched in METLIN. Observed fragments: 237.2218, 311.2451, 313.2478, 385.2751, 387.2931, 621.4864, 623.5019, and 697.5170. According to this fragmentation pattern *m/z* = 968.7563, $[M+NH_4]^+$, was identified as TAG (16:1, 22:5, 22:6) ($m/z_{theoretical}$ = 968.7702).

**Identification of *m/z* = 970.7711.** Retention time = 65.8. MS/MS fragments obtained were searched in METLIN. Observed fragments: 239.2339, 311.2325, 313.2668, 623.4865, and 625.5071. According to this fragmentation pattern *m/z* = 970.7711, $[M+NH_4]^+$, was identified as TAG (16:0, 22:5, 22:6) ($m/z_{theoretical}$ = 970.7858).

**Identification of *m/z* = 974.8006.** Retention time = 66.8. MS/MS fragments obtained were searched in METLIN. Observed fragments: 287.2409, 313.2490, 341.3001, 627.5388, 653.5474, and 673.5159. According to this fragmentation pattern *m/z* = 974.8006, $[M+NH_4]^+$, was identified as TAG (18:0, 20:4, 22:5) ($m/z_{theoretical}$ = 974.8171).

**Identification of *m/z* = 976.8316.** Retention time = 66.6. MS/MS fragments obtained were searched in METLIN. Observed fragments: 287.2206, 315.2629, 341.3003, 385.2575, 627.5134, 655.5522 and 675.5183. According to this fragmentation pattern *m/z* = 976.8316, $[M+NH_4]^+$, was identified as TAG (18:0, 20:4, 22:4) ($m/z_{theoretical}$ = 976.8328).

**Identification of *m/z* = 998.8025.** Retention time = 65.5. MS/MS fragments obtained were searched in METLIN. Observed fragments: 265.2552, 311.2293, 339.2726, 389.3103, 649.5160, 653.5508, and 699.5405. According to this fragmentation pattern *m/z* = 998.8025, $[M+NH_4]^+$, was identified as TAG (18:1, 22:4, 22:6) ($m/z_{theoretical}$ = 998.8171).

**Identification of *m/z* = 1000.8153.** Retention time = 66.6. MS/MS fragments obtained were searched in METLIN. Observed fragments: 267.2586, 311.2295, 315.2659, 341.3016, 385.2612, 651.5368, 655.5633, and 699.5352. According to this fragmentation pattern *m/z* = 1000.8153, $[M+NH_4]^+$, was identified as TAG (18:0, 22:4, 22:6) ($m/z_{theoretical}$ = 1000.8328).

Identification of Representative Members from Major Lipid Families Identified During Targeted Lipidomics

**Identification of *m/z* = 313.2743.** Retention time =46.8. MS/MS fragments obtained were searched in METLIN. Observed fragments: 239.2411. According to this fragmentation pattern *m/z* = 313.2743, $[M+H-H_2O]^+$, was identified as MAG (16:0) ($m/z_{theoretical}$ = 313.2747).

**Identification of *m/z* = 369.3521.** Retention time = 56.8. MS/MS fragments obtained were searched in METLIN. Observed fragments: 135.1169, 161.1326, 201.1654, 215.1805, 229.1942, and 257.2260. According to this fragmentation pattern *m/z* = 369.3521, $[M+H-H_2O]^+$, was identified as cholesterol ($m/z_{theoretical}$ = 369.3516).

**Identification of *m/z* = 494.3247.** Retention time = 42.3. MS/MS fragments obtained were searched in METLIN. Observed fragments: 184.0702, 237.2324, and 258.1002. According to this fragmentation pattern *m/z* = 494.3247, $[M+H]^+$, was identified as LPC (16:1) ($m/z_{theoretical}$ = 494.3241).

**Identification of *m/z* = 500.2777.** Retention time = 36.1. MS/MS fragments obtained were searched in METLIN. Observed fragments: 78.9569, 140.0298, and 303.2311. According to this fragmentation pattern *m/z* = 500.2777, $[M-H]^-$, was identified as LPE (20:4) ($m/z_{theoretical}$ = 500.2783).

**Identification of *m/z* = 524.2988.** Retention time = 32.4. MS/MS fragments obtained were searched in METLIN. Observed fragments: 78.9525, 152.9909, and 283.2860. According to this fragmentation pattern *m/z* = 524.2988, $[M-H]^-$, was identified as LPS (18:0) ($m/z_{theoretical}$ = 524.2994).

**Identification of *m/z* = 536.5048.** Retention time = 63.4. MS/MS fragments obtained were searched in METLIN. Observed fragments: 237.2207, 280.2629, 298.2774, and 488.4596. According to this fragmentation pattern *m/z* = 536.5048, $[M-H]^-$, was identified as ceramide (16:0) ($m/z_{theoretical}$ = 536.5048).

**Identification of *m/z* = 577.5196.** Retention time = 60.3. MS/MS fragments obtained were searched in METLIN. Observed fragments: 237.2208, 267.2688, and 341.3042. According to this fragmentation pattern *m/z* = 577.5196, $[M+H-H_2O]^+$, was identified as DAG (16:1/18:0) or DAG (34:1) ($m/z_{theoretical}$ = 577.5190).

**Identification of *m/z* = 599.3196.** Retention time = 37.8. MS/MS fragments obtained were searched in METLIN. Observed fragments: 78.9591, 152.9968, 241.0072, and 283.2646. According to this fragmentation pattern *m/z* = 599.3196, $[M-H]^-$, was identified as LPI(18:0) ($m/z_{theoretical}$ = 599.3202).

**Identification of *m/z* = 673.4808.** Retention time = 62.0. MS/MS fragments obtained were searched in METLIN. Observed fragments: 78.9587, 96.9687, 152.9958, 255.2353, 281.2544, 409.2488, and 435.2455. According to this fragmentation pattern *m/z* = 673.4808, $[M-H]^-$, was identified as PA (16:0/18:1) or PA (34:1) ($m/z_{theoretical}$ = 673.4814).

**Identification of *m/z* = 673.5900** Retention time = 62.6. MS/MS fragments obtained were searched in METLIN. Observed fragments: 205.2133, 305.2439, and 369.3494. According to this fragmentation pattern *m/z* = 673.5900, $[M+Na]^+$, was identified as CE (18:1) ($m/z_{theoretical}$ = 673.5894).

**Identification of *m/z* = 698.5492.** Retention time = 62.0. MS/MS fragments obtained were searched in METLIN. Observed fragments: 181.0856, 237.2203, 280.2592, and 536.4945. According to this fragmentation pattern *m/z* = 698.5492, $[M-H]^-$, was identified as Hexosyl ceramide (16:0) ($m/z_{theoretical}$ = 698.5576).

**Identification of *m/z* = 720.5907.** Retention time = 57.9 MS/MS fragments obtained were searched in METLIN. Observed fragments: 184.0736, 239.2402, and 482.3604. According to this fragmentation pattern *m/z* = 720.5907, $[M+H]^+$, was identified as PC (O-16:0/16:0) or PC (32:0) ($m/z_{theoretical}$ = 720.5902).

**Identification of *m/z* = 744.5543.** Retention time = 55.8 MS/MS fragments obtained were searched in METLIN. Observed fragments: 78.9616, 140.0129, 281.2484, 283.2622, and 480.3144. According to this fragmentation pattern *m/z* = 744.5543, $[M-H]^-$, was identified as PE (18:1/18:0) or PE (36:1) ($m/z_{theoretical}$ = 744.5549).

**Identification of *m/z* = 750.5438.** Retention time = 53.6. MS/MS fragments obtained were searched in METLIN. Observed fragments: 78.9578, 140.0096, 267.2812, 303.2348, and 464.3257. According to this fragmentation pattern *m/z* = 750.5438, $[M-H]^-$, was identified as PE (O-18:1/20:4) or PE (O-38:5) ($m/z_{theoretical}$ = 750.5443).

**Identification of *m/z* = 760.5856.** Retention time = 57.8. MS/MS fragments obtained were searched in METLIN. Observed fragments: 184.0715, 258.1157, 239.2522, 265.2449, 496.3395, and 522.3541. According to this fragmentation pattern *m/z* = 760.5856, $[M+H]^+$, was identified as PC (16:0/18:1) or PC (34:1) ($m/z_{theoretical}$ = 760.5851).

**Identification of *m/z* = 770.5336.** Retention time = 51.1. MS/MS fragments obtained were searched in METLIN. Observed fragments: 78.9611, 96.9657, 152.9961, 281.2493, 417.2357, and 506.3067. According to this fragmentation pattern *m/z* = 770.5336, $[M-H]^-$, was identified as PS (O-18:2/18:1) or PS (O-36:3) ($m/z_{theoretical}$ = 770.5341).

**Identification of *m/z* = 786.5285.** Retention time = 44.0. MS/MS fragments obtained were searched in METLIN. Observed fragments: 78.9607, 96.9731, 152.9958, 281.2485, 417.2405, and 522.2882. According to this fragmentation pattern *m/z* = 786.5285, $[M-H]^-$, was identified as PS (18:1/18:1) or PS (36:2) ($m/z_{theoretical}$ = 786.5291).

**Identification of *m/z* = 809.5180.** Retention time = 49.7. MS/MS fragments obtained were searched in METLIN. Observed fragments: 78.9638, 96.9688, 152.9958, 241.0188, and 255.2297. According to this fragmentation pattern *m/z* = 809.5180, $[M-H]^-$, was identified as PI (16:0/16:0) or PI (32:0) ($m/z_{theoretical}$ = 809.5186).